Resonance Raman Spectra of Two Isomeric Dioxygen Adducts of Iron(II) Porphyrins and π-Cation Radical and Nonradical Oxoferryl Porphyrins Produced in Dioxygen Matrices: Simultaneous Observation of More Than Seven Oxygen Isotope Sensitive Bands

Leonard M. Proniewicz,[†] Insook Rhee Paeng,[‡] and Kazuo Nakamoto*[,‡]

Contribution from the Todd Wehr Chemistry Building, Marquette University, Milwaukee, Wisconsin 53233, and Regional Laboratory of Physicochemical Analyses and Structural Research, Jagiellonian University, 30-060 Kracow, ul. Karasia 3, Poland.
Received September 4, 1990

Abstract: The resonance Raman (RR) spectra of "base-free" dioxygen adducts of Fe(TPP), Fe(TPP-d_8), Fe(TMP), Fe(OEP), and Fe(TPFPP) in $^{16}O_2$, $^{18}O_2$, and scrambled O_2 ($^{16}O_2$:$^{16}O^{18}O$:$^{18}O_2$=1:2:1) matrices at ~30 K have been measured with 406.7-nm excitation. The ν(O–O), ν(Fe–O_2) and δ(FeOO) of "end-on" adducts were observed at 1223–1188, 516–486, and 349–337 cm^{-1}, respectively, whereas the ν(O–O) and ν_a(Fe–O) of "side-on" adducts were located at 1105–1102 and 411–405 cm^{-1}, respectively. In addition, some side-on adducts exhibit the ν_s(Fe–O) coupled with porphyrin modes in the 700–500 cm^{-1} region. The band assignments of end-on isomers were confirmed by $^{56}Fe/^{54}Fe$ substitution as well as by normal coordinate calculations. During RR measurements, two oxoferryl species were formed as a result of homolytic cleavage of the O–O bond by laser irradiation. One exhibits the ν(FeO) at 861–853 cm^{-1} (compound A), while the other (less stable species) shows it at 815–809 cm^{-1} (compound B). While the former originates in the well-established base-free, nonradical oxoferryl porphyrin, the latter is attributed to a new oxoferryl species in which the porphyrin ring assumes an a_{2u} π-cation radical form. A mechanism has been proposed to account for the formation of these oxoferryl porphyrins in an O_2 matrix.

Introduction

Elucidation of the molecular mechanism of dioxygen binding and its biological activation by heme proteins has been the focus of sustained attention for over two decades.[1-4] Considerable interest has been centered on dioxygen adducts of iron porphyrins and oxoferryl species. The most intensely investigated dioxygen complexes are oxyhemoglobin (HbO_2) and oxymyoglobin (MbO_2), which are respiratory proteins to transport and store molecular oxygen, respectively.[1] Dioxygen adducts have also been found as intermediates in the catalytic cycles of cytochromes c oxidase,[5] cytochromes P-450,[3] and peroxidases (compound III).[6] On the other hand, the presence of oxoferryl porphyrins as a transient, unstable species has been confirmed or postulated in the enzymatic cycles of horseradish peroxidases,[7-9] cytochromes c oxidase,[10] cytochromes P-450,[3] and catalases.[2,9]

Many model complexes that reversibly bind O_2 have been developed to understand the influence of the steric, electronic, and environmental factors on dioxygen binding in native heme proteins. These model systems include "unprotected" porphyrins with different peripheral substituent groups as well as "protected" porphyrins[11,12] such as picket-fence and capped porphyrins. It is, therefore, important to establish spectroscopic probes to compare the structure and bonding of the key molecular fragments such as the iron–dioxygen group between heme proteins and their model systems.

The utility of resonance Raman (RR) spectroscopy to study dioxygen binding to heme proteins and their model compounds has been demonstrated by many investigators.[13-15] In favorable cases, the presence of charge-transfer transitions accessible by available laser lines facilitates direct resonant enhancement of vibrational modes representing the metal–dioxygen linkage. Thus, spectral features associated with ν(O–O) and ν(Fe–O_2) (ν stretching) vibrations have been identified in RR spectra and definitive assignments of these key modes made with the aid of isotopically labeled compounds. Historically, the first observation of the ν(Fe–O_2) band was made for HbO_2 at 567 cm^{-1} by Brunner.[16] Burke et al.[17] obtained a virtually identical frequency in the RR spectrum of the oxyiron "picket-fence" porphyrin imidazole complex. However, this assignment was questioned by Benko and Yu[18] on the basis of the "isotopic zigzag pattern," which was similar to that obtained for the δ(FeCO) (δ bending) of HbCO. These researchers preferred to assign it to the δ(FeOO) rather than to the ν(Fe–O_2). However, Bajdor et al.[19] have shown that the original assignment of the ν(Fe–O_2) by Brunner is correct since Fe(Pc)O_2 (Pc, phthalocyanato dianion) exhibits the ν(Fe–O_2) and δ(FeOO) at 488 and 279 cm^{-1}, respectively. Thus far, attempts to observe the ν(O–O) of heme proteins containing an axial histidine ligand by RR spectroscopy have not been successful. This is anticipated from MO calculations that predict the Fe–O_2

[†] Jagiellonian University.
[‡] Marquette University.

(1) Dickerson, R. E.; Geis, I. *Hemoglobin: Structure, Function, Evolution and Pathology*; Benjamin/Cummings: Menlo Park, CA, 1983.
(2) Caughey, W. S.; Choc, M. G.; Houtchens, R. A. In *Biochemical and Clinical Aspects of Oxygen*; Caughey, W. S., Ed.; Academic Press: New York, 1978; p 1.
(3) Ortiz de Montellano, P. R., Ed. *Cytochrome P-450; Structure, Mechanism and Biochemistry*; Plenum Press: New York, 1986.
(4) Mathews, F. S. *Prog. Biophys. Mol. Biol.* **1985**, *45*, 1.
(5) Hill, B. C.; Greenwood, C.; Nicholls, P. *Biochim. Biophys. Acta* **1986**, *853*, 91.
(6) Nakajima, R.; Yamazaki, I. *J. Biol. Chem.* **1987**, *262*, 2576.
(7) Hashimoto, S.; Tatsuno, Y.; Kitagawa, T. *Proc. Jpn. Acad.* **1984**, *60B*, 345.
(8) Terner, J.; Sitter, A. J.; Reczek, C. M. *Biochim. Biophys. Acta* **1985**, *828*, 73.
(9) Frew, J. E.; Jones, P. In *Advances in Inorganic and Bioinorganic Mechanisms*; Academic Press: New York, 1984; Vol. 3, p 175.
(10) Blair, D. F.; Witt, S. N.; Chan, S. I. *J. Am. Chem. Soc.* **1985**, *107*, 7389.
(11) Collman, J. P.; Halbert, T. R.; Suslick, K. S. In *Metal Ions in Biology*; Spiro, T. G., Eds.; John Wiley: New York, 1980; Vol. 2, p 1.
(12) Morgan, M.; Dolphin, D. *Struct. Bonding (Berlin)* **1987**, *64*, 116.
(13) Yu, N.-T.; Kerr, E. A. In *Biological Applications of Raman Spectroscopy*; Spiro, T. G., Ed.; Wiley-Interscience: New York, 1987; Vol. 3, p 39.
(14) Spiro, T. G. In *Iron Porphyrins*; Lever, A. B. P., Gray, H. B., Eds.; Addison-Wesley: Reading, MA, 1983; Vol. 2, p 89.
(15) Kitagawa, T.; Ozaki, Y. *Struct. Bonding (Berlin)* **1987**, *64*, 71.
(16) Brunner, H. *Naturwissenschaften* **1974**, *61*, 129.
(17) Burke, J. M.; Kincaid, J. R.; Peters, S.; Gagne, R. R.; Collman, J. P.; Spiro, T. G. *J. Am. Chem. Soc.* **1978**, *100*, 6083.
(18) Benko, B.; Yu, N.-T. *Proc. Natl. Acad. Sci. U.S.A.* **1983**, *80*, 7042.
(19) Bajdor, K.; Oshio, H.; Nakamoto, K. *J. Am. Chem. Soc.* **1984**, *106*, 7273.

0002-7863/91/1513-3294$02.50/0

charge-transfer transition of HbO_2 in the range 1300–780 nm.[20] However, the ν(O–O) was observed near 1140 cm^{-1} for oxygenated cytochrome P-450[21] and its model compounds containing axial thiolate ligands.[22] Very recently, we[23] have made simultaneous observation of the ν(O–O) and ν(Fe–O_2) of Fe(TPP)O_2 at 1195 and 509 cm^{-1}, respectively, in an O_2 matrix at ~30 K with 406.5-nm excitation.

In the last decade, efforts have been made to locate the ν(FeO) of oxoferryl species in RR spectra. The main difficulty in detecting this mode arises from the very limited stability of the oxoferryl complexes. We[24,25] first succeeded in the observation and characterization of the ν(FeO) (852 cm^{-1}) of OFe(TPP), OFe(OEP), and OFe(Salen), which were formed by laser photolysis of the corresponding dioxygen adducts in O_2 matrices at ~15 K. Since then, several groups of researchers observed the ν(FeO) of nonradical oxoferryl porphyrins and their π-cation radical species in heme proteins and their model complexes.[8,26-29] In the case of horseradish peroxidase compound I (HRP-I), however, RR data presented by different researchers[28b,29b,c] were inconsistent due to its inherent reactivity and photoliability, and this has prevented unambiguous characterization of its π-cation radical complex.

The present research is a continuation of our earlier IR[30] and RR[23-25] studies on dioxygen adducts of iron porphyrins and their oxoferryl derivatives, which are formed in low-temperature dioxygen matrices. Here, we report simultaneous observation of the RR spectra of two isomeric dioxygen adducts (isomers I and II) of Fe(TPP), ^{54}Fe(TPP), Fe(TPP-d_8), Fe(TMP), and Fe(OEP), which were produced via cocondensation reactions of these iron porphyrins with $^{16}O_2$, $^{18}O_2$, and "scrambled O_2" ($^{16}O_2$:$^{16}O^{18}O$:$^{18}O_2$ = 1:2:1), and of their two oxoferryl species (compounds A and B), which were obtained by laser photolysis of these dioxygen adducts. In total, we observed more than seven oxygen isotope sensitive bands in a single dioxygen matrix and proposed the most probable assignments for these bands. In the case of the most acidic porphyrin Fe(TPFPP), however, we were able to observe only those of one dioxygen adduct (isomer I) and one oxoferryl species (compound A) in a single matrix. Based on this and other information, we concluded that the two isomeric dioxygen adducts are end-on and side-on types and that the two oxoferryl porphyrins are nonradical and π-cation radical types. Finally, we proposed a mechanism that leads to the formation of these oxoferryl species in low-temperature O_2 matrices.

Experimental Section

Compound Preparation. 5,10,15,20-Tetraphenylporphine (H_2TPP), 2,3,7,8,12,13,17,18-octaethylporphine (H_2OEP), and 5,10,15,20-tetramesitylporphine (H_2TMP) were purchased from Midcentury, Posen, IL, whereas 5,10,15,20-tetrakis(pentafluorophenyl)porphine iron(III) chloride (Fe(TPFPP)Cl) was purchased from Aldrich Chemical Co. To remove tetraphenylchlorin contamination, H_2TPP was refluxed with 2,3-dichloro-5,6-dicyano-1,4-benzoquinone (DDQ) in toluene, extracted with sodium dithionite, and then chromatographed over dry aluminum with chloroform.[31] H_2OEP and H_2TMP were free from reduced porphyrins and used without further purification. The deuteriated analogue

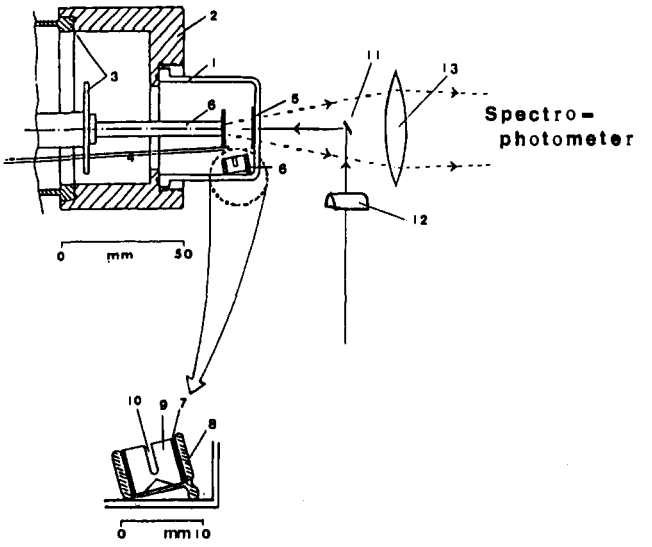

Figure 1. Schematic drawing of matrix isolation apparatus used for RR measurements: 1, glass envelope; 2, aluminum sleeve; 3, refrigerator; 4, gas line; 5, steel screen; 6, cold tip; 7, aluminum radiation shield; 8, Pyrex cup; 9, spectroscopic-grade spark graphite rod; 10, Pyrex capillary tube with sample; 11, small mirror; 12, cylindrical lens; 13, collecting lens.

of tetraphenylporphine (H_2TPP-d_8) was synthesized by refluxing benzaldehyde and deuteriated pyrrole in deuteriated propionic acid (CH_3C-H_2COOD) and purified as described above. The metal was incorporated into H_2TPP, H_2TPP-d_8, and H_2OEP by refluxing the porphyrins in glacial acetic acid containing ferric chloride.[32] In the case of H_2TMP, ferrous chloride was added to refluxing dimethylformamide under a nitrogen atmosphere.[33] Fe(por)(pip)$_2$ (por = porphyrin (TPP, TPP-d_8, TMP, OEP, and TPFPP); pip = piperidine) were synthesized by reduction of Fe(por)Cl with piperidine in refluxing chloroform under a nitrogen atmosphere.[34]

The gases $^{16}O_2$ (over 99% pure, AmeriGas) and $^{18}O_2$ (~97% ^{18}O atom, Monsanto Research) were used without further purification. Samples of scrambled dioxygen ($^{16}O_2$:$^{16}O^{18}$:$^{18}O_2$ = 1:2:1) were prepared by electrical discharge in an equimolar mixture of $^{16}O_2$ and $^{18}O_2$. Ozone produced during this process was decomposed by activated 4A molecular sieves, which were added to the reaction flask. The exact mixing ratio of the isotopic dioxygens was determined by Raman spectroscopy.

Spectral Measurement. The samples for RR measurements were prepared by using the laser-heated miniature oven technique.[35] Figure 1 illustrates the improved design of the miniature oven and optical arrangement used for this work. First, Fe(por)(pip)$_2$ was placed into a Pyrex capillary tube, which was fitted into the hole (10) drilled at the center of a spectroscopic-grade spark graphite rod (8-mm diameter, 5 mm long) (9). The rod was surrounded by an aluminum radiation shield (7) to reduce heat loss, and the whole oven was inserted into a Pyrex cup (8). Then the miniature oven thus assembled was placed under the copper cold tip (6), and a laser beam was aimed at the graphite rod to heat it up to ~450 K under vacuum (~10^{-5} Torr) to remove adsorbed water and dissociate coordinated piperidine from the complex. Depending on the compound used in the experiment, the oven temperature was raised to 500–650 K to vaporize the "base-free" Fe(por) and cocondense it with dioxygen on the surface of the cold tip (6), which was cooled to ~30 K by a CTI Model 21 closed-cycle helium cryocooler (3). A small steel screen (5) was placed inside the glass envelope (1) to avoid the deposition of Fe(por) in the optical path. After the cocondensation reaction was completed, the screen was removed for RR measurements. To study highly unstable species formed in an O_2 matrix, back-scattering geometry[36] (11) was set up with a cylindrical lens (12) to produce a line focus on the sample surface. Furthermore, fast codeposition of dioxygen with Fe(por) (15–20 min) relative to that used in our previous study (4–6 h)[23] resulted in a dense and thin matrix, which provided close contact with the cold tip surface, thus preventing thermal decomposition of the dioxygen adduct via highly efficient cooling. Additionally, the low laser

(20) Case, D. A.; Huynh, B. H.; Karplus, M. *J. Am. Chem. Soc.* **1979**, *101*, 4433.
(21) Bangcharoenpaurpong, O.; Rizos, A. K.; Champion, P. M.; Jollie, D.; Sligar, S. G. *J. Biol. Chem.* **1986**, *261*, 8089.
(22) Chottard, G.; Schappacher, M.; Ricard, L.; Weiss, R. *Inorg. Chem.* **1984**, *23*, 4557.
(23) Wagner, W.-D.; Paeng, I. R.; Nakamoto, K. *J. Am. Chem. Soc.* **1988**, *110*, 5565.
(24) Bajdor, K.; Nakamoto, K. *J. Am. Chem. Soc.* **1984**, *106*, 3045.
(25) Proniewicz, L. M.; Bajdor, K.; Nakamoto, K. *J. Phys. Chem.* **1986**, *90*, 1760.
(26) Gold, A.; Jayaraji, K.; Doppelt, P.; Weiss, R.; Chottard, G.; Bill, E.; Ding, X.; Trautwein, A. X. *J. Am. Chem. Soc.* **1988**, *110*, 5756.
(27) Kean, R. T.; Oertling, W. A.; Babcock, G. T. *J. Am. Chem. Soc.* **1987**, *109*, 2185.
(28) (a) Hashimoto, S.; Teraoka, J.; Inubushi, T.; Yonetani, T.; Kitagawa, T. *J. Biol. Chem.* **1986**, *261*, 11110. (b) Palaniappan, V.; Terner, J. *J. Biol. Chem.* **1989**, *264*, 16046.
(29) (a) Kincaid, J. R.; Schneider, A. J.; Paeng, K.-J. *J. Am. Chem. Soc.* **1989**, *111*, 735. (b) Paeng, K.-J.; Kincaid, J. R. *J. Am. Chem. Soc.* **1988**, *110*, 7913. (c) Ogura, T.; Kitagawa, T. *Rev. Sci. Instrum.* **1988**, *59*, 1316.
(30) Watanabe, T.; Ama, T.; Nakamoto, K. *J. Phys. Chem.* **1984**, *88*, 440.
(31) Rousseau, K.; Dolphin, D. *Tetrahedron Lett.* **1974**, *48*, 4251.
(32) Chang, C. K.; Di Nello, R. R.; Dolphin, D. In *Inorganic Synthesis*; Busch, D. H., Ed.; Wiley: New York, 1981; Vol. 20, p 157.
(33) Kobayashi, H.; Higuchi, T.; Kaizu, Y.; Osada, M.; Aoki, M. *Bull. Chem. Soc. Jpn.* **1975**, *48*, 3137.
(34) Epstein, L. M.; Straub, D. K.; Maricondi, C. *Inorg. Chem.* **1967**, *6*, 1720.
(35) Scheuermann, W.; Nakamoto, K. *Appl. Spectrosc.* **1978**, *32*, 251.
(36) Shriver, D. F.; Dunn, J. B. R. *Appl. Spectrosc.* **1974**, *28*, 319.

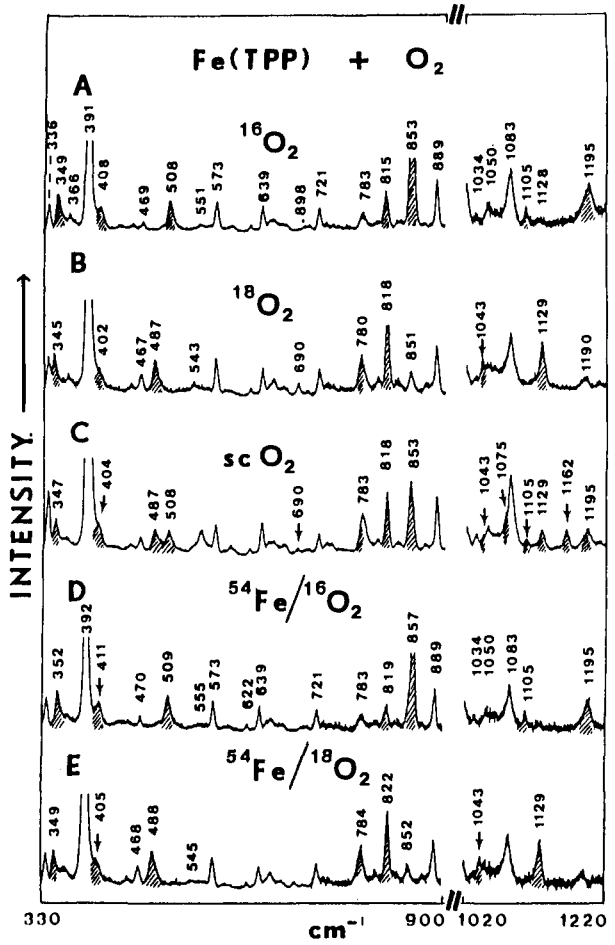

Figure 2. RR spectra of Fe(TPP) cocondensed with dioxygen at ~30 K (406.7-nm excitation): (A) $^{16}O_2$, (B) $^{18}O_2$, (C) scrambled O_2 ($^{16}O_2$:$^{16}O^{18}O$:$^{18}O_2$ = 1:2:1), (D) $^{54}Fe/^{16}O_2$, and (E) $^{54}Fe/^{18}O_2$. Shaded bands are oxygen isotope sensitive.

power and short scanning time used in these measurements enabled us to detect RR bands of unstable species that were not possible to observe in previous experiments.

RR spectra were measured on a Spex Model 1403 double monochromator equipped with a Hamamatsu R928 photomultiplier tube and a Spex DM1B computer. Excitation at 406.7 nm was made with a Coherent Model Innova 100-K3 Krypton ion laser. For standard measurements, the power at the sample was kept ~3 mW. Accuracy of the frequency reading was ±1 cm^{-1}. A spectral band path of 4 cm^{-1} was used routinely.

Results and Discussion

(1) Fe(TPP) in O_2 Matrices. (A) Dioxygen Adducts. According to our previous IR studies,[30] the cocondensation product of Fe(TPP) with dioxygen at ~15 K consists of two isomeric dioxygen adducts of Fe(TPP)O_2. The major product exhibiting the ν(O–O) at 1195 cm^{-1} has been assigned to an "end-on" isomer (isomer I), while the minor one with the ν(O–O) at 1106 cm^{-1} has been attributed to a "side-on" isomer (isomer II). The latter is unstable and converted into the end-on isomer by raising the temperature up to 110 K. Recently,[23] we were able to observe not only the ν(O–O) (1195 cm^{-1}) but also the ν(Fe–O_2) (509 cm^{-1}) of the end-on isomer in the RR spectrum of Fe(TPP)O_2 using 406.7 nm excitation.

Figure 2 shows the RR spectra of the cocondensation products of Fe(TPP) with O_2 at ~30 K obtained by 406.7-nm excitation (~3 mW). Upon laser irradiation, the corresponding oxoferryl species OFe(TPP) is formed as a result of photolytic cleavage of the O–O bond of Fe(TPP)O_2 in O_2 matrices.[24,25] Thus, the bands due to the dioxygen adducts become weaker, whereas those associated with the oxoferryl complexes become stronger during the course of RR measurements. These spectral changes proceed further as the laser power is increased and/or the irradiation time is lengthened. To minimize this photodecomposition, we recorded the RR spectra by dividing the 330–1220 cm^{-1} region into four 200 cm^{-1} sections (330–530, 530–730, 700–900 and 1020–1220 cm^{-1}) so that a fresh spot was exposed in the laser focus for each measurement.

In addition to typical TPP macrocycle vibrations, Figure 2 shows a number of bands that are sensitive to $^{16}O_2/^{18}O_2$ and/or $^{56}Fe/^{54}Fe$ substitution (these isotope-sensitive bands are shaded in this and subsequent figures). When Fe(TPP) vapor is cocondensed with $^{16}O_2$, new bands appear at 349, 408, 508, 815, 853, 1105, and 1195 cm^{-1} (trace A), and these bands are shifted to 345, ~402, 487, 780, 818, 1043, and 1129 cm^{-1}, respectively (trace B), upon $^{16}O_2/^{18}O_2$ substitution. Some of these bands have already been assigned. Thus, the bands at 1195 (1129) and 1105 (1043) cm^{-1} are due to the ν(O–O) of the end-on isomer (isomer I) and side-on isomer (isomer II), respectively, of the Fe(TPP)O_2.[30] Hereafter, the number in parentheses indicates the frequency of the corresponding $^{18}O_2$ analogue. When a similar experiment is carried out with a 1:2:1 isotopic mixture of $^{16}O_2/^{16}O^{18}O/^{18}O_2$ (scrambled dioxygen), additional bands appear at 1162 and 1075 cm^{-1} (shoulder), i.e., exactly in the middle between those of the $^{16}O_2$ and $^{18}O_2$ adducts for each isomer (trace C). Thus, these bands are readily assigned to the ν($^{16}O^{18}O$) of isomers I and II, respectively. It should be noted that the RR frequencies of these ν(O–O) are in excellent agreement with those previously observed in IR spectra.[30] In addition, their $^{16}O_2/^{18}O_2$ isotopic shift values are in good agreement with those expected for a diatomic harmonic oscillator. In trace C, the intensity pattern of the ν(O–O) bands for isomer I is close to 1:1:1 instead of 1:2:1, which is expected for the scrambled dioxygen used in our experiments. This apparent anomaly is due to the presence of the porphyrin bands at ~1190 and 1128 cm^{-1}, which overlap the ν(^{16}O–^{16}O) and ν(^{18}O–^{18}O), respectively.[23] The relative intensity of the ν(^{16}O–^{18}O) bands of isomer II at 1075 cm^{-1} is also anomalous because it is partially overlapped by the strong porphyrin band at ~1083 cm^{-1}.

In addition to the ν(O–O) vibration, the end-on adduct exhibits two other modes (ν(Fe–O_2) and δ(FeOO)). The former is expected to appear near 500 cm^{-1} and downfield by ~23 cm^{-1} on $^{16}O_2/^{18}O_2$ substitution.[19] Furthermore, it should show two bands when scrambled dioxygen is employed since the ν(Fe–$^{16}O^{18}O$) and ν(Fe–$^{18}O^{16}O$) are close to the ν(Fe–$^{16}O^{16}O$) and ν(Fe–$^{18}O^{18}O$), respectively.[37] On the other hand, the δ(FeOO) is expected to be below 400 cm^{-1} and downshift only several wave numbers on $^{16}O_2/^{18}O_2$ substitution.[19] Although four δ(FeOO) bands are anticipated for the scrambled dioxygen, only one broad band was observed because of the small isotopic shifts (6–7 cm^{-1}).

As seen in Figure, 2, three bands are observed at 349, 408, and 508 cm^{-1} (trace A), which are shifted to 345, ~402 and 487 cm^{-1}, respectively, upon $^{16}O_2/^{18}O_2$ substitution (trace B). When scrambled dioxygen is used (trace C), two bands appear at 347 and ~404 cm^{-1}, while the bands at 508 and 487 cm^{-1} appear with equal intensity. We assign the bands at 508 (487) and 349 (345) cm^{-1} to the ν(Fe–O_2) and δ(FeOO) of the end-on isomer, respectively. The newly observed band at 408 (402) cm^{-1} is attributed to the ν_a(Fe–O) of the side-on isomer. In the side-on structure, the Fe–O stretching vibration tends to couple with porphyrin vibrations due to its tilted Fe–O linkages with respect to the porphyrin plane. Thus, several weak oxygen isotope sensitive bands in the 530–730 cm^{-1} region may be assigned to the ν_s(Fe–O) coupled with porphyrin modes.

All of the above assignments were further confirmed by $^{56}Fe/^{54}Fe$ substitution. As shown in traces D and E of Figure 2, the δ(FeOO) and ν(Fe–O_2) of isomer I at 349 (345) and 508 (487) cm^{-1} are shifted upfield to 352 (349) and 509 (488) cm^{-1}, respectively, while the ν_a(Fe–O) of isomer II is also shifted upfield from 408 (~402) to 411 (~405) cm^{-1}. As expected, the ν(O–O) vibrations show no $^{56}Fe/^{54}Fe$ shifts. Table I gives the results of normal coordinate calculations on a triatomic FeOO fragment of the end-on isomer (isomer I). The good agreement between

(37) Duff, L. L.; Appelman, E. H.; Shriver, D. F.; Klotz, I. M. *Biochem. Biophys. Res. Commun.* **1979**, *90*, 1098.

Table I. Comparison of Observed and Calculated Frequencies of End-on FeO_2 Moiety in $Fe(TPP)O_2$ (cm^{-1})[a]

	obsd (calcd)		
	ν(O–O)	ν(Fe–O_2)	δ(FeOO)
$Fe(TPP)^{16}O_2$	1195	508	349
	(1199)	(508)	(350)
$Fe(TPP)^{18}O_2$	1129	487	345
	(1127)	(485)	(343)
$^{54}Fe(TPP)^{16}O_2$	1195	509	352
	(1199)	(509)	(353)

[a] The frequencies were calculated by assuming the following parameters: R(O–O) = 1.25 Å, R(Fe–O) = 2.00 Å, ϕ(FeOO) = 137 (see ref 11), K(O–O) = 6.55 mdyn/Å, K(Fe–O) = 2.00 mdyn/Å, H(FeOO) = 0.27 mdyn/Å.

the observed and calculated frequencies provides further support for our assignments. Previously, we[19] assigned the bands at 488 and 279 cm^{-1} in the RR spectrum of $FePcO_2$ to the ν(Fe–O_2) and δ(FeOO), respectively, based on similar calculations. Thus, we conclude that the bands near 500 cm^{-1} are due to the ν(Fe–O_2), although other researchers[18] assigned them to the δ(FeOO).

(B) Oxoferryl Complexes. As demonstrated previously,[24,25] oxoferryl porphyrin (OFe(TPP)) is formed via laser photolysis of $Fe(TPP)O_2$ in O_2 matrices. This species is well-characterized as a nonradical oxoferryl complex (OFe(IV)(TPP) (compound A)) and exhibits the ν(FeO) as a strong feature at 853 (818) cm^{-1} in the RR spectrum (Figure 2A). As expected, only two ν(FeO) bands are observed at 853 and 818 cm^{-1} when scrambled dioxygen is used (trace C), and both bands show a 4 cm^{-1} upfield shift upon $^{56}Fe/^{54}Fe$ substitution (traces D and E).

Careful examination of our data reveals the presence of another band at 815 cm^{-1}, which is also sensitive to $^{16}O/^{18}O$ and $^{56}Fe/^{54}Fe$ substitutions. In trace A, this band overlaps on the porphyrin band at 812 cm^{-1}. Upon $^{16}O_2/^{18}O_2$ substitution, it is shifted to 780 cm^{-1}, where it again overlaps on the porphyrin band at 783 cm^{-1} (trace B). With scrambled dioxygen, three bands are observed at 853, 818, and 783 cm^{-1} (trace C). The middle band is an overlap of two oxygen isotope sensitive bands at 815 and 818 cm^{-1}, which are further overlapped by the porphyrin band at 812 cm^{-1}. The fact that no new band is seen between 818 and 783 cm^{-1} in trace C rules out the possibility of assigning the 815 (780) cm^{-1} band to the ν(O–O) of (TPP)FeO_2Fe(TPP). Furthermore, such a peroxo-bridged dimer should exhibit the ν_s(Fe–O) near 574 (547) cm^{-1}.[38] The 815 (780) cm^{-1} band cannot be attributed to the ν_s(Fe–O) of the μ-oxo dimer (TPP)FeOFe(TPP) since it should show the ν_s(Fe–O) at 366 cm^{-1}.[39] This is also supported by the observation that the 815 (780) cm^{-1} band appears in the spectrum of the cocondensation product of Fe(TMP) with O_2 (Figure 6), even though Fe(TMP) cannot form the μ-oxo dimer due to steric hindrance of the methyl groups. Furthermore, the μ-oxo complex is stable at room temperature, while the band in question disappears at ~45 K or with a higher laser power. Finally, these bands cannot be attributed to the dioxo species $Fe(TPP)(O)_2$ since their ν_s(OFeO) frequencies should not be sensitive to $^{56}Fe/^{54}Fe$ substitution (traces D and E). Thus, we assign the band at 815 (780) cm^{-1} to the second OFe(TPP) species (compound B), the structure of which will be discussed later. All of the observed frequencies and assignments of oxygen isotope sensitive bands are listed in Table II.

(2) Fe(TPP-d_8) in O_2 Matrices. (A) Dioxygen Adducts. Next, we carried out similar experiments with Fe(TPP-d_8) to minimize the overlap of Fe(TPP) bands on oxygen isotope sensitive bands.

Figure 3 shows the RR spectra of Fe(TPP-d_8) cocondensed with $^{16}O_2$ (trace A), $^{18}O_2$ (trace B), and scrambled dioxygen (trace C) at ~30 K. In the 1020–1220 cm^{-1} region, the bands at 1195 (1129) and 1105 (1043) cm^{-1} are assigned to the ν(O–O) of isomers I and II of Fe(TPP-d_8)O_2, respectively (traces A and B).

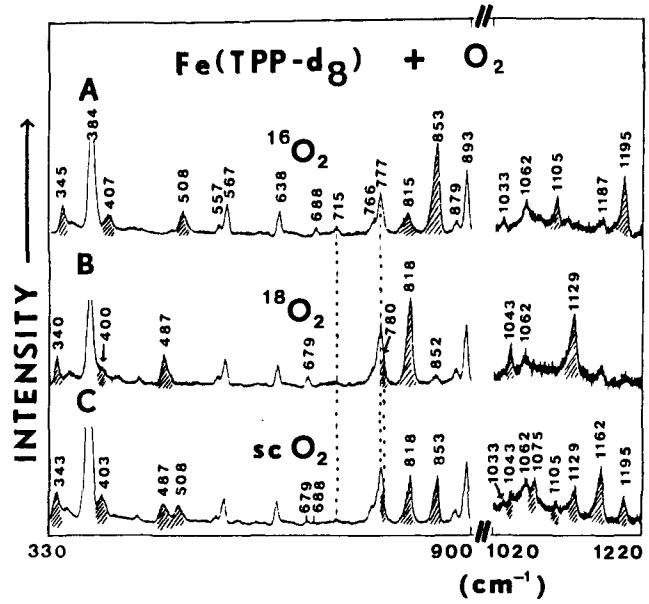

Figure 3. RR spectra of Fe(TPP-d_8) cocondensed with dioxygen at ~30 K (406.7-nm excitation): (A) $^{16}O_2$, (B) $^{18}O_2$, and (C) scrambled O_2. Shaded bands are oxygen isotope sensitive.

As mentioned in the preceding section, the TPP macrocycle exhibits bands at ~1190, 1128, and ~1083 cm^{-1}, which interfere with the ν(O–O), resulting in intensity perturbation and frequency uncertainty. Since these bands are shifted below 1000 cm^{-1} by the deuteriation, all the ν(O–O) bands can now be observed without interference. Thus, trace C shows six ν(O–O) bands at 1195, 1162, 1129, 1105, 1075, and 1043 cm^{-1}, with the intensity pattern close to 1:2:1 for both isomers as expected from the composition of the scrambled dioxygen.

In the low-frequency region, a very strong Fe(TPP) band at 391 cm^{-1} (Figure 2) has now been shifted to 384 cm^{-1} so that the ν_s(Fe–O) frequency of isomer II can be determined with certainty; this band is located at 407, ~400, and 403 cm^{-1} for the $^{16}O_2$, $^{18}O_2$, and $^{16}O^{18}O$ adducts, respectively. As discussed in the preceding section, two oxygen isotope sensitive bands at 508 (487) and 345 (340) $cm1^{-1}$ are due to the ν(Fe–O_2) and δ(FeOO), respectively, of isomer I. The δ(FeOO) of Fe(TPP-d_8) is ~4 cm^{-1} lower than that of $Fe(TPP)O_2$, indicating the effect of vibrational coupling with one of the TPP-d_8 modes. Such coupling is known to occur frequently between vibrations of bound dioxygen and those of the base ligand, porphyrin, or solvent and leads to unexpected frequency shifts and intensity perturbations of bound dioxygen modes.[40-42] It is to be noted that the weak band at 688 cm^{-1} is shifted to 679 cm^{-1}, while the band at ~715 cm^{-1} becomes much broader by $^{16}O_2/^{18}O_2$ substitution. As discussed in the preceding section, this suggests the presence of vibrational coupling between the ν_s(Fe–O) and some porphyrin modes in isomer II.

(B) Oxoferryl Complexes. In traces A and B of Figure 3, the presence of the oxoferryl species (compound A) is manifested by its characteristic ν(FeO) bands at 853 and 818 cm^{-1}, which appear with equal intensities in trace C (scrambled dioxygen). As discussed in the preceding section, the ν(FeO) of OFe(TPP) (compound B) shifts from 815 cm^{-1} to ~780 cm^{-1} upon $^{16}O_2/^{18}O_2$ substitution. Although this band is now partly overlapped by the porphyrin band at 777 cm^{-1}, its presence in trace B can be inferred from the apparent intensification of the 777 cm^{-1} band relative to the porphyrin band at 893 cm^{-1}.

Figure 4 shows the RR spectra (406.7 nm excitation) of cocondensation products of Fe(TPP-d_8) with $^{16}O_2$ at ~30 K obtained by increasing laser power from 0.2 (trace A) to 8.0 mW (trace

(38) Paeng, I. R.; Shiwaku, H.; Nakamoto, K. *J. Am. Chem. Soc.* **1988**, *110*, 1995.
(39) Burke, J. M.; Kincaid, J. R.; Spiro, T. G. *J. Am. Chem. Soc.* **1978**, *100*, 6077.
(40) Tsubaki, M.; Yu, N.-T. *Proc. Natl. Acad. Sci. U.S.A.* **1981**, *78*, 3581.
(41) Odo, J.; Imai, H.; Kyuno, E.; Nakamoto, K. *J. Am. Chem. Soc.* **1988**, *110*, 742.
(42) (a) Proniewicz, L. M.; Nakamoto, K.; Kincaid, J. R. *J. Am. Chem. Soc.* **1988**, *110*, 4541. (b) Proniewicz, L. M.; Kincaid, J. R. *J. Am. Chem. Soc.* **1990**, *112*, 675.

Table II. Observed Frequencies of Dioxygen Adducts and Ferryl Complexes in O_2 Matrices (cm^{-1})[a]

		Fe(TPP)	^{54}Fe(TPP)	Fe(TPP-d_8)	Fe(TMP)	Fe(OEP)	Fe(TPFPP)
$\nu(O_2)$	I	1195 (1129)	1195 (1129)	1195 (1129)	1188 (1120)	1192 (1126)	1223 (1158)
	II	1105 (1043)	1105 (1043)	1105 (1043)	1102 (c)	1104 (1042)	c
$\nu(Fe-O_2)$	I	508 (487)	509 (488)	508 (487)	516 (492)	509 (486)	486 (469)
$\nu_s(Fe-O)$	II	698 (690)[b]	c	688 (679)[b]	c	622 (603)[b]	c
		551 (543)[b]	c				
$\delta(FeOO)$	I	349 (345)	352 (349)	345 (340)	343 (338)		337 (333)
$\nu_a(Fe-O)$	II	408 (~402)	411 (405)	407 (400)	411 (c)	405 (393)	c
$\nu(Fe=O)$	A	853 (818)	857 (822)	853 (818)	854 (819)	853 (818)	861 (825)
	B	815 (780)	819 (784)	815 (~780)	809 (~776)	811 (777)	c

[a] Numbers in parentheses indicate the corresponding frequencies of the $^{18}O_2$ or ^{18}O analogues. [b] Coupled with porphyrin modes. [c] Not observed.

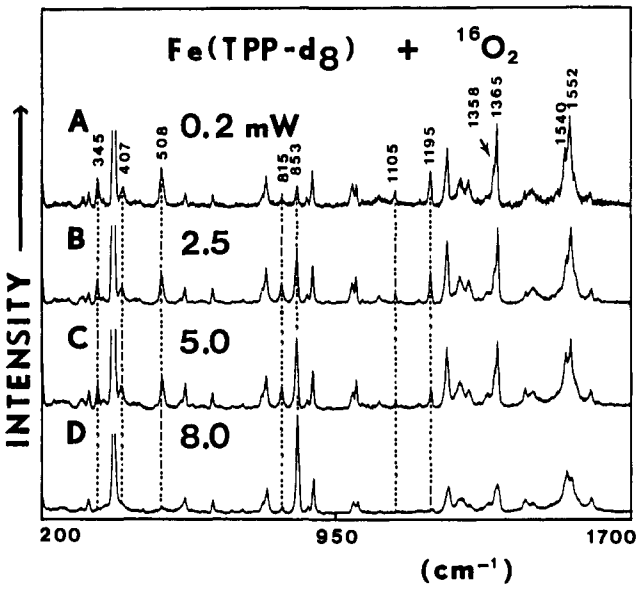

Figure 4. RR spectra of Fe(TPP-d_8) cocondensed with $^{16}O_2$ at ~30 K (406.7-nm excitation): (A) 0.2, (B) 2.5, (C) 5.0, and (D) 8.0 mW.

D). Each trace is a composite of the spectra obtained in the four regions 200–600, 600–1000, 1000–1400, and 1300–1700 cm^{-1}, which were recorded separately. Several bands characteristic of the two isomeric dioxygen adducts are observed at 1195, 1105, 508, 407, and 345 cm^{-1}. In trace A, the intensities of the bands associated with isomer I (1195, 508, and 345 cm^{-1}) are strong, whereas those due to isomer II (1105 and 407 cm^{-1}) are weak. When laser power is increased to 2.5 (trace B) and 5.0 mW (trace C), the bands associated with both dioxygen adducts become weak, whereas those of the oxoferryl complexes at 853 and 815 cm^{-1} become strong. In trace D, all the bands due to the dioxygen adducts disappear completely, while the ν(FeO) at 853 cm^{-1} becomes extremely strong although the second ν(FeO) at 815 cm^{-1} becomes substantially weaker on going from trace C to D. Similar change is noted for the ν_4 band of the dioxygen adducts at 1358 cm^{-1}, which disappears slowly upon increasing the laser power. The strong feature at ~1365 cm^{-1} is due to the ν_4 of the nonradical oxoferryl species (compound A). It is rather difficult, however, to assign the spectra in the 1560–1540 cm1–1 region since these bands consist mainly of the $\nu(O_2)$ of free dioxygen, which overlaps the ν_2 bands of several species.

Figure 5A, B, C, and D shows plots of the intensity versus irradiation time for the bands at 815, 853, 1105, and 1195 cm^{-1}, respectively. In each figure, traces a, b, c, d, and e indicate the results obtained with laser power of 0.2, 1.0, 2.5, 5.0, and 8.0 mW, respectively. As is seen in Figure 5A, the intensity of the 815 cm^{-1} band (compound B) increases slowly at low power (traces a and b), whereas at higher power (traces c, d, and e) it increases rapidly. The rate of formation of this complex is proportional to the laser power used in the experiment. For example, when the laser power of 8.0 mW is applied on the surface of the cold tip, formation of compound B is completed within ~2 min and then it starts to decompose exponentially after several minutes (trace e). This is in contrast to the 853 cm^{-1} band (compound A) that gains intensity

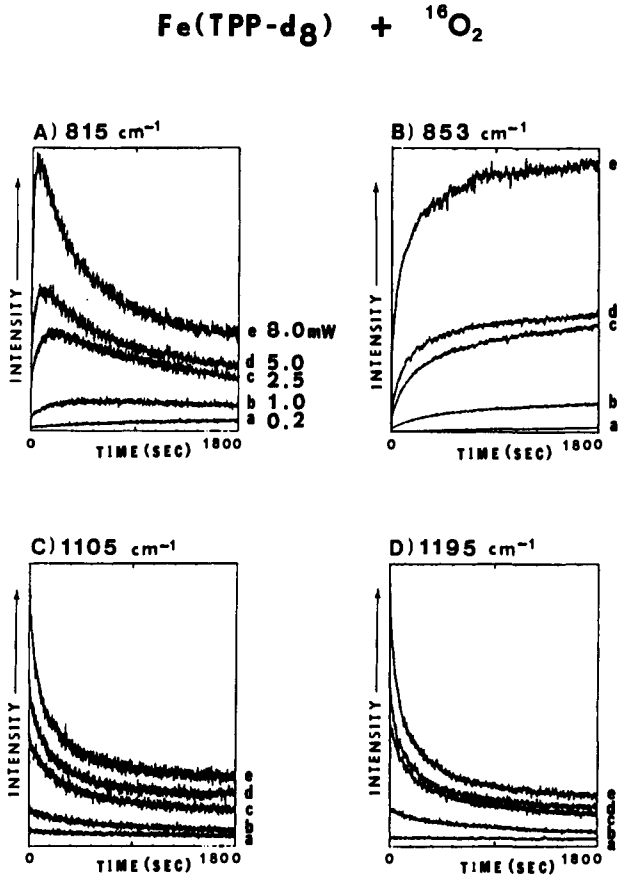

Figure 5. Relative intensity vs time of the two ν(FeO) of oxyferryl species and two $\nu(O_2)$ of dioxygen adducts of Fe(TPP-d_8) cocondensed with $^{16}O_2$ at ~30 K (406.7-nm excitation). Traces a, b, c, d, and e were obtained with laser power 0.2, 1.0, 2.5, 5.0, and 8.0 mW, respectively, for the bands at (A) 815 cm^{-1}, (B) 853 cm^{-1}, (C) 1105 cm^{-1}, and (D) 1195 cm^{-1}.

with time for every laser power used (Figure 5B); traces c, d, and e show rapid formation of compound A during the first 5 min and completion after ~20 min. As seen in Figure 5C and D, the ν(O–O) bands of the dioxygen adducts at 1105 (isomer II) and 1195 (isomer I) cm^{-1} show only slight decreases in intensity at lower laser power (traces a and b) but marked exponential decreases with higher laser power. In these plots, the 1552 cm^{-1} band was used as the internal standard. Since its intensity decreases at higher laser power (Figure 4), proper intensity correction should be made for plots d and e in each figure. Such corrections were not made, however, in the plots shown in Figure 5 since the shapes of these plots remain essentially unchanged even with these corrections. In similar experiments with $^{18}O_2$, the $\nu(^{18}O-^{18}O)$ of free dioxygen appeared at ~1460 cm^{-1}, and the results obtained after the intensity corrections were essentially the same as those presented in Figure 5.

(3) Fe(TMP) in O_2 Matrices. (A) Dioxygen Adducts. Traces A, B, and C of Figure 6 show the RR spectra of cocondensation products of Fe(TMP) with $^{16}O_2$, $^{18}O_2$, and scrambled dioxygen, respectively. The bands at 1188, 516, and 343 cm^{-1} (trace A)

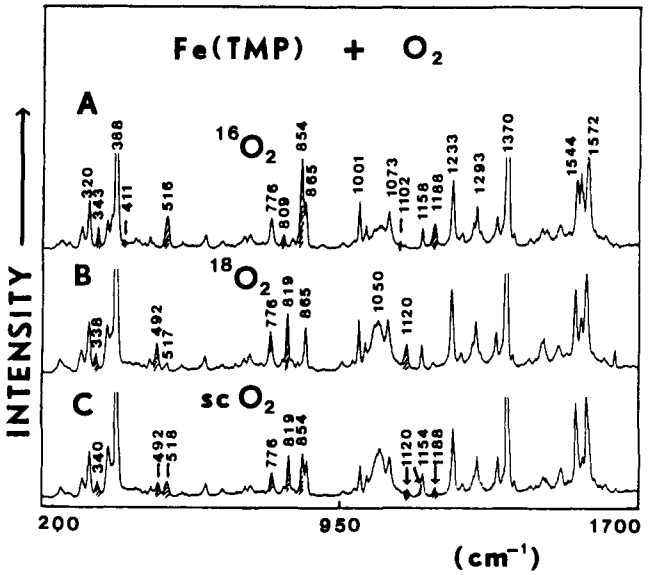

Figure 6. RR spectra of Fe(TMP) cocondensed with dioxygen at ~30 K (406.7-nm excitation): (A) $^{16}O_2$, (B) $^{18}O_2$, and (C) scrambled O_2. Shaded bands are oxygen isotope sensitive.

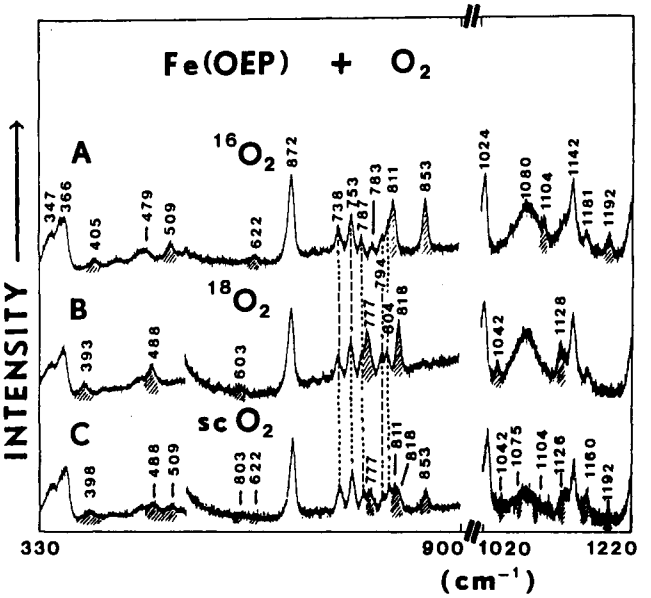

Figure 7. RR spectra of Fe(OEP) cocondensed with dioxygen at ~30 K (406.7-nm excitation): (A) $^{16}O_2$, (B) $^{18}O_2$, and (C) scrambled O_2. Shaded bands are oxygen isotope sensitive.

are readily assigned to the ν(O–O), ν(Fe–O_2) and δ(FeOO) of the end-on isomer (isomer I). These bands are shifted to 1120, 492, and 338 cm^{-1}, respectively, upon $^{16}O_2/^{18}O_2$ substitution (trace B). The shifts observed for the ν(O–O) (68 cm^{-1}) and ν(Fe–O_2) (24 cm^{-1}) are in good agreement with those predicted for a diatomic harmonic oscillator. The bands associated with isomer II were observed only as weak shoulders when the spectra were recorded with the standard 4 cm^{-1} band-pass. With use of a narrow slit (2.5 cm^{-1} band-pass), however, it was possible to locate the ν(O–O) and ν_a(Fe–O) at 1102 and 411 cm^{-1}, respectively (trace A). In an $^{18}O_2$ matrix (trace B), both bands are shifted to lower frequencies and hidden under strong porphyrin bands at ~1050 and 388 cm^{-1}, respectively. In a scrambled dioxygen matrix (trace C), the bands due to isomer I are clearly seen but those of isomer II are practically indiscernible due to their low intensities. The $\nu(^{16}O–^{18}O)$ is observed as a shoulder (~1154 cm^{-1}) on the porphyrin band at 1158 cm^{-1}. Two bands at 516 and 492 cm^{-1} are readily assigned to the ν(Fe–$^{16}O_2$) and ν(Fe–$^{18}O_2$), respectively, while that centered at ~340 cm^{-1} is an overlap of the δ(FeOO) of all the isotopic dioxygen adducts (isomer I).

(B) Oxoferryl Complexes. Similar to OFe(TPP), OFe(TMP) is formed when Fe(TMP)O_2 is irradiated with a 406.7-nm line. Formation of this species is demonstrated by the appearance of a strong ν(FeO) band at 854 (819) cm^{-1}. The observed shift of 35 cm^{-1} by $^{16}O/^{18}O$ substitution is in good agreement with that expected for a diatomic harmonic oscillator. The second ν(FeO) band at 809 cm^{-1} overlaps the porphyrin band at 807 cm^{-1}. Upon $^{16}O_2/^{18}O_2$ substitution, this band shifts to ~776 cm^{-1} (trace B), where it is again overlapped on the porphyrin band at 776 cm^{-1}. The spectral pattern obtained for the scrambled dioxygen (trace C) can be explained as an overlap of the spectra shown in traces A and B.

(4) Fe(OEP) in O_2 Matrices. (A) Dioxygen Adducts. Figure 7 shows the RR spectra of Fe(OEP) cocondensed with $^{16}O_2$ (trace A), $^{18}O_2$ (trace B), and scrambled dioxygen (trace C) at ~30 K. Traces A and B show the presence of two oxygen isotope sensitive bands at 1192 (1126) (isomer I) and 1104 (1042) cm^{-1} (isomer II). When scrambled dioxygen is used (trace C), additional bands due to the $\nu(^{16}O–^{18}O)$ of these isomers appear at 1160 and ~1075 cm^{-1}, although the presence of the latter is obscured by the appearance of the broad band at 1080 cm^{-1}. The 1080 cm^{-1} band disappears when the matrix is warmed or O_2 is diluted with Ar (Figure 9). Although the nature of this band is not clear, it must be due to a specific porphyrin–O_2 interaction that occurs only in pure O_2 matrix at 30 K. In the 530–330 cm^{-1} region, the ν(Fe–O_2) of isomer I at 509 cm^{-1} is shifted to 486 cm^{-1} upon $^{16}O_2/^{18}O_2$ substitution. Unfortunately, its δ(FeOO) is masked by the strong porphyrin bands at 340–370 cm^{-1}. The band at 405 cm1–^{1} is due to the ν_a(Fe–O) of isomer II and is shifted to 393 cm^{-1} by $^{16}O_2/^{18}O_2$ substitution. It should be noted that the observed shift of 12 cm^{-1} is 2 times larger than that of the ν_a(Fe–O) of Fe(TPP)O_2. When scrambled dioxygen is used, a broad nonresolved band appears with a center at 398 cm^{-1} (trace C). Although we cannot locate the ν_s(Fe–O) of isomer II definitively, the band at 622 cm^{-1} (trace A) may be attributed to this mode since it shifts to 603 cm^{-1} (trace B) by $^{16}O_2/^{18}O_2$ substitution. However, the observed isotopic shift (19 cm^{-1}) is still smaller than that expected for a diatomic harmonic oscillator (27 cm^{-1}) because of vibrational coupling with a porphyrin mode near 580 cm^{-1}.

(B) Oxoferryl Complexes. As shown previously,[25] the bands at 853 (818) and 811 (777) cm^{-1} are assigned to the ν(FeO) of compounds A and B, respectively. With scrambled dioxygen (trace C), four ν(FeO) bands are observed at 853, 818, 811, and 777 cm^{-1} with almost equal intensity (the bands at 804 and 794 cm^{-1} are due to porphyrin vibrations). These ν(FeO) bands exhibit similar intensity versus irradiation time relatinships observed for OFe(TPP-d_8) (Figure 5). The intensity of the ν(FeO) at 811 (777) cm^{-1} relative to that at 853 (818) cm^{-1} is much higher in OFe(OEP) than in the TPP, TPP-d_8, and TMP analogues. This is probably due to either one or a combination of the following two factors: (1) the OFe(OEP) (compound B) is much more stable than those of the other porphyrins and (2) the FeO charge-transfer transition of OFe(OEP) may be closer to the exciting line (406.7 nm) than those of the other porphyrins. Such a trend was noted previously for the Soret band maxima of OEP complexes, which are at shorter wavelength than those of the corresponding TPP complexes (e.g., 378 and 417 nm for Fe(OEP)Cl and Fe(TPP)Cl, respectively).[43]

(5) Fe(TPFPP) in O_2 Matrices. (A) Dioxygen Adducts. Figure 8 shows the RR spectra of Fe(TPFPP) cocondensed with $^{16}O_2$ (trace A), $^{18}O_2$ (trace B), and scrambled dioxygen (trace C) at ~30 K. In the 1000–1200 cm^{-1} region, the ν(O–O) of isomer I appears at 1223 cm^{-1} (trace A) as a shoulder on the 1217 cm^{-1} band of the porphyrin and is shifted to 1158 cm^{-1} upon $^{16}O_2/^{18}O_2$ substitution (trace B), where it is partly hidden by the 1164 cm^{-1} band of the porphyrin. With scrambled dioxygen (trace C), an additional band due to the $\nu(^{16}O–^{18}O)$ of this isomer is observed at 1189 cm^{-1}. The presence of these bands is seen more clearly in the spectra drawn on the expanded scale. It was not possible, however, to locate the ν(O–O) of isomer II. It is either masked

(43) Czernuszewicz, R. S.; Su, Y. O.; Stern, M. K.; Macor, K. A.; Kim, D.; Groves, J. T.; Spiro, T. G. *J. Am. Chem. Soc.* **1988**, *110*, 4158.

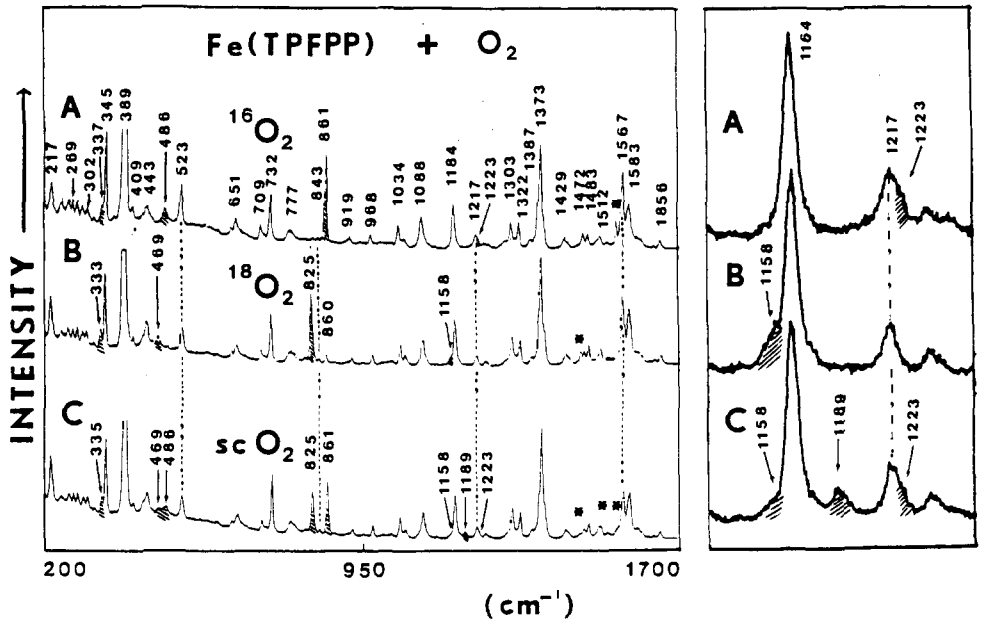

Figure 8. RR spectra of Fe(TPFPP) cocondensed with dioxygen at ~30 K (406.7-nm excitation): (A) $^{16}O_2$, (B) $^{18}O_2$, and (C) scrambled O_2. Shaded bands are oxygen isotope sensitive. Bands marked by asterisks are due to the $\nu(O_2)$ of free dioxygen.

by the porphyrin band or too weak to be observed (the ν(O–O) of isomer II is generally much weaker than that of isomer I). The bands at 486 (469) and 337 (333) cm^{-1} (trace A) are readily assignable to the ν(Fe–O_2) and δ(FeOO) of isomer I, respectively. However, low-frequency vibrations of isomer II were not observed.

It is interesting to note that the ν(O–O) (1223 cm^{-1}) and ν(Fe–O_2) (486 cm^{-1}) of Fe(TPFPP)O_2 are the highest and the lowest, respectively, among the iron porphyrins that we have studied thus far; the former is 35 cm^{-1} higher and the latter is 30 cm^{-1} lower than that of Fe(TMP)O_2. In general, the more acidic the porphyrinato ligand, the less electron density on the metal ion and the less π-back-bonding from the metal to dioxygen, resulting in a weaker metal–O_2 bond and a stronger O–O bond. TPFPP is highly acidic since the electron density on the porphyrin ring is reduced markedly due to strong electron-withdrawing property of the fluorine atoms on the phenyl rings. This trend is reversed in TMP since the methyl groups are weakly electron-donating. Accordingly, the order of the ν(O–O) of isomer I becomes Fe(TPFPP)O_2 (1223 cm^{-1}) > Fe(TPP)O_2 (1195 cm^{-1}) > Fe(OEP)O_2 (1192 cm^{-1}) > Fe(TMP)O_2 (1188 cm^{-1}), which reflects the order of ligand basicity.

(B) Oxoferryl Complexes. Similar to the other porphyrins, OFe(TPFPP) is formed upon irradiation of Fe(TPFPP)O_2 with a 406.7-nm line. A strong ν(FeO) band appears at 861 cm^{-1} (trace A), which is shifted to 825 cm^{-1} by $^{16}O_2/^{18}O_2$ substitution (trace B). With scrambled dioxygen, two ν(FeO) bands appear at 861 and 825 cm^{-1} with almost equal intensity. This ν(FeO) frequency (compound A) is the highest among the ν(FeO) observed thus far. This is readily explained by the strong electron-withdrawing effect of the pentafluorophenyl groups, which makes the porphyrin ring highly electron deficient and increases the π-donor property of the oxo ligand. In contrast to the other porphyrins, the second ν(FeO) band (compound B) was not observed in the case of Fe(TPFPP).

(6) Structures of Two Forms of Oxoferryl Porphyrins. As described in the preceding sections, we observed two ν(FeO) bands near 853 and 810 cm^{-1} for OFe(TPP), OFe(TMP), and OFe(OEP) and only one ν(FeO) band at 861 cm^{-1} for OFe(TPFPP). The band near 853 cm^{-1} (compound A) has already been shown to be the ν(FeO) of the five-coordinate nonradical oxoferryl porphyrin, which involves a low spin (S = 1) Fe atom with formal oxidation state IV.[25] This frequency is much higher than that of the ν(Fe–O_2) of five-coordinate dioxygen adducts in O_2 matrices (516–486 cm^{-1}), the ν_s(Fe–O) of the five-coordinate peroxo-bridged species (574 cm^{-1})[38] and the ν(Fe–O_2) of a six-coordinate oxyiron picket-fence porphyrin imidazole complex (567 cm^{-1}).[17] Its high frequency clearly indicates a multiple bond character of the FeO bond. In our earlier work,[25] we formulated it as a triple bond (IV)Fe≡O^{2-}, which involves one σ [d_{z^2}(Fe)–P_z(O)] and two π [d_{xz}(Fe)–P_x(O) and d_{yz}(Fe)–P_y(O)] bonds. Formation of these two π-bonds stems from the equivalence of the p and d orbitals in the x and y directions. However, these π-bonds are expected to be weak since two electrons occupy two antibonding π-orbitals consisting of the d_π(Fe) and $2p_\pi$(O) overlap,[43] thus reducing bond order from 3 to 2. This is in agreement with the results of recent MO calculations on the Fe–O bond of oxoferryl porphyrins.[44,45] Thus, the oxoferryl bonds are conventionally expressed as Fe(IV)=O. The $d_{z^2} \rightarrow p_z$ σ-bonding in addition to the π-bonding gives a force constant of 5.32 mdyn/Å for the ν(FeO) vibration located at 852 cm^{-1}. This π-bonding contributes to the shortening of the FeO bond relative to that in dioxygen adducts and μ-oxo dimers.

Five- and six-coordinate oxoferryl complexes can also be formed in solutions at low temperature. In noncoordinating solvents such as tetrahydrofuran (THF) or toluene, the ν(FeO) is ~10 cm^{-1} lower[26,38] than those in O_2 matrices because of weak interaction with the solvent. The ν(FeO) of oxoiron "picket-fence" porphyrin in THF solution is further lowered (829 cm^{-1}) by the polarity effect of the pivalamido groups surrounding the oxo ligand.[46] When a coordinating ligand such as dimethylformamide (DMF) is used as the solvent or a strong base ligand is present in solution, the ν(FeO) is shifted to the 818–828 cm^{-1} range for unprotected porphyrins and is further lowered ~10 cm^{-1} in picket-fence porphyrin due to the added polarity effect of the cavity.[26,46,47] The weakening of the Fe–O bond in these six-coordinate complexes is attributed to the axial ligand effect; the oxo ligand is a σ- as well as a π-donor; thus, the axial ligand at the trans position to the oxoferryl group hinders electron donation from the oxo ligand to the iron atom, resulting in weakening of both σ- and π-bonds.[24] Thus, the stronger the electron-donating ability of the trans ligand, the lower the ν(FeO).[26]

The most puzzling feature in the RR spectra reported here is the observation of a new ν(FeO) band at 815–809 cm^{-1} (compound B). This band is generally weak and partially overlapped by the porphyrin band for Fe(TPP), Fe(TPP-d_8), or Fe(TMP) but is

(44) Yamamoto, S.; Teraoka, J.; Kashiwagi, H. J. Chem. Phys. 1988, 88, 303.
(45) Hanson, L. K.; Chang, C. K.; Davis, M. S.; Fajer, J. J. Am. Chem. Soc. 1981, 103, 663.
(46) Schappacher, M.; Chottard, G.; Weiss, R. J. Chem. Soc., Chem. Commun. 1986, 93.
(47) Balch, A. L.; Chan, Y. W.; Cheng, R. J.; La Mar, G. M.; Latos-Grazynski, L.; Renner, M. W. J. Am. Chem. Soc. 1984, 106, 7779.

Table III. Vibrational Frequencies of OV(OEP), OFe(OEP), and Their π-Cation Radicals (cm^{-1})

mode	symmetry (D_{4h})	assignments[a]	OV(OEP)[b]	OV(OEP^{+})[b]	Δ[c]	OFe(OEP)[d]	OFe(OEP^{+})[d]	Δ[c]
ν_{10}	B_{1g}	$\nu(C_\alpha-C_m)$	1628	1621	−7	1653	1636	−17
ν_2	A_{1g}	$\nu(C_\beta-C_\beta)$	1580	1601	+21	1595	1578	−17
ν_3	A_{1g}	$\nu(C_\alpha-C_m)_{sym}$	1494			1507	1516	+9
ν_4	A_{1g}	ν(pyr half-ring)$_{sym}$	1376	1359	−17	1380	1372	−8

[a] Reference 59. [b] Reference 61. [c] Δ = frequency shifts upon radical formation. [d] This work.

strong and distinct for Fe(OEP), while it is not observed for Fe(TPFPP). It is shifted downfield ~35 cm^{-1} by $^{16}O/^{18}O$ substitution and upfield ~4 cm^{-1} by $^{56}Fe/^{54}Fe$ substitution. When scrambled dioxygen is used, only two bands are observed at 815–809 and 780–776 cm^{-1} without any oxygen isotope sensitive band between them. Furthermore, its intensity versus irradiation time relationship (Figure 5A) is markedly different from that of compound A (Figure 5B).

In Section 1B, we considered several nonferryl structures that might be responsible for the 815–809 cm^{-1} band and ruled out the possibilities of assigning it to the ν(O–O) of the peroxo-bridged dimer, the ν_s(Fe–O) of the μ-oxo dimer, and the ν_s(O=Fe=O) of the dioxo species. We have also considered several other possibilities and ruled them out for the following reasons: (1) The bands cannot be attributed to the ν_s(Fe–O) of the dioxygen adduct (isomer II) since the intensity versus irradiation time relationship is different from that of the ν(O–O) at 1105 cm^{-1} (Figure 5). (2) The bands cannot be associated with iron(III) porphyrin *N*-oxide[48] since the observed frequency (810 cm^{-1}) suggests the Fe–O bond order to be close to 2, which is higher than that expected for the Fe–O(N) bond of such an *N*-oxide. (3) As stated earlier, several six-coordinate ferryl complexes in solution exhibit the ν(FeO) at 829–818 cm^{-1}.[26,27,46] In our experiment, the possibility of forming OFe(por)(pip) is remote since the base ligand has been completely dissociated from Fe(por) by heating Fe(por)$(pip)_2$ at ~250 °C for ~5 h under high vacuum (~5×10^{-4} Torr) while keeping the graphite oven away from a cold tip in the rear part of the matrix isolation apparatus (Figure 1). (4) We considered the possibility of oxoferryl porphyrins having high-spin Fe atoms. If this were the case, the spin-state-sensitive bands such as ν_2 and ν_{10} would be altered when the matrix containing both isomers (A and B) was warmed. No such spectral changes were observed. (5) Finally, we considered oxoferryl porphyrins having appreciable interaction with the matrix environment. If so, the relative intensities of the two ν(FeO) bands should change when dioxygen is diluted by Ar (O_2:Ar = 1:15, 1:35, and 1:150). This was not the case, however. As discussed below, we conclude that the ν(FeO) at 815–809 cm^{-1} is most probably due to the oxoferryl porphyrin π-cation radical formed in O_2 matrices. The fact that only nonradical oxoferryl species is formed by Fe(TPFPP) provides further support since its porphyrin core is too electron deficient to stabilize the π-cation radical species.

Under D_{4h} symmetry of the metalloporphyrin, there are two highest occupied molecular orbitals (HOMO) of a_{1u} and a_{2u} symmetry that are nearly degenerate.[49,50] The exact energies of these two orbitals depend on the nature of the peripheral substituents, axial ligation, temperature, and solvent.[45] However, EPR measurements[51] as well as theoretical calculations[52,53] indicate that the A_{1u} and A_{2u} states are mixed as a general rule and the pseudo-Jahn–Teller effect provides a mechanism for this mixing.[54] Nevertheless, the removal of an electron from a porphyrin core leads to a π-cation radical with a predominantly $^2A_{1u}$ or $^2A_{2u}$ ground electronic state. The unpaired charge density in an $^2A_{1u}$ π-cation radical resides primarily on the α- and β-pyrrole carbon atoms, whereas in an $^2A_{2u}$ π-cation radical a much greater spin density is on the pyrrole nitrogen and meso carbon atoms.[52,53,55] Thus, metal complexes of *meso*-arylporphyrin such as M(TPP) or M(TMP) tend to form an $^2A_{2u}$-type π-cation radical, whereas β-pyrrole-substituted alkylporphyrins such as MOEP tend to form an $^2A_{1u}$-type π-cation radical in the absence of the axial ligand.[56–58]

RR spectra show characteristic features associated with π-cation radical formation that are markedly different from those of the parent complexes.[56–58] In M(OEP) complexes, the ν_2 and ν_{11} modes exhibit large upfield shifts while the ν_3, ν_4, and ν_{10} modes show modest downfield shifts upon radical formation. In M(TPP) complexes, however, the pattern of the RR frequency shifts upon radical formation is different from that of the M(OEP) complexes; ν_2 shows a large downfield shift, although the downfield shifts of ν_4 and ν_{10} are similar to that of M(OEP) (for complete normal mode analysis of M(OEP) and M(TPP) complexes, see refs 59 and 60, respectively). Thus, we have chosen the ν_2 as a marker of the radical type. This band is mainly due to the $\nu(C_\beta-C_\beta)$ pyrrole ring vibration.[59,60] Since the $C_\beta-C_\beta$ interaction is bonding, removal of an electron from M(TPP) (A_{2u} radical) weakens the $C_\beta-C_\beta$ bond, thus shifting the ν_2 downfield. The opposite trend holds for M(OEP) (A_{1u} radical) since the $C_\beta-C_\beta$ interaction is antibonding.

All the RR spectra presented in this work exhibit very complex patterns in the high-frequency region. In all but Fe(TPFPP) complexes, two dioxygen adducts and two oxoferryl species are formed in a single matrix and structure-sensitive porphyrin bands of these four complexes are expected to appear in a close range. Thus, it is extremely difficult to locate the peaks due to the π-cation radical in the high-frequency region. Additional complications arise from the fact that, upon π-cation radical formation, the intensities of all the porphyrin modes decrease dramatically.[29] Thus, the bands due to the π-cation radical may be either too weak to be observed or easily masked by the bands from other porphyrin complexes. Moreover, these porphyrin bands may be much weaker than that of the ν(FeO) of the π-cation radical.[29] Thus, we were not able to locate them in the present study with the exception of OFe(OEP^{+}) (see Figure 9), where marked changes were observed in the high-frequency region upon increasing the laser power.

Figure 9 shows a series of RR spectra of Fe(OEP) cocondensed with $^{18}O_2$/Ar with increasing laser power and irradiation time on going from trace A to D. As already shown in Figure 7B, the bands at 1126 and 1042 cm^{-1} are due to the ν(O–O) of isomers I and II whereas those at 818 and 777 cm^{-1} are due to the ν(FeO) of nonradical oxoferryl porphyrin and oxoferryl porphyrin in question, respectively. It is seen that both ν(O–O) bands become weaker on going from trace A to D and disappear completely in trace D, whereas the ν(FeO) at 818 cm^{-1} becomes stronger on going from trace A to B, with no appreciable changes in going from trace B to D. The effect of laser power on the 777 cm^{-1} band is markedly different from that on the 818 cm^{-1} band; the former is the strongest in trace B and disappears completely in trace D.

(48) Groves, J. T.; Watanabe, Y. *J. Am. Chem. Soc.* **1988**, *110*, 8443.
(49) Gouterman, M. In *The Porphyrins*; Dolphin, D., Ed.; Academic Press, New York, 1978; Vol III.
(50) Spellane, P. J.; Gouterman, M.; Antepas, A.; Kim, S.; Liu, Y. C. *Inorg. Chem.* **1980**, *19*, 386.
(51) Fujita, E.; Chang, C. K.; Fajer, J. *J. Am. Chem. Soc.* **1985**, *107*, 7665.
(52) Kashiwagi, H.; Obara, S. *Int. J. Quantum Chem.* **1981**, *20*, 843.
(53) Spangler, D.; Maggiora, G. M.; Shipman, L. L.; Christofferson, R. E. *J. Am. Chem. Soc.* **1977**, *99*, 7478.
(54) Siebrand, W.; Zgierski, M. In *Excited States*; Lim, E. C., Ed.; Academic Press: New York, 1979; Vol. 4, p 1.
(55) Fajer, J.; Davis, M. S. In *The Porphyrins*; Dolphin, D., Ed.; Academic Press: New York, 1979; Vol. 4, p 197.
(56) Czernuszewicz, R. S.; Macor, K. A.; Li, X.-Y.; Kincaid, J. R.; Spiro, T. G. *J. Am. Chem. Soc.* **1989**, *111*, 3860.
(57) Oertling, W. A.; Salehi, A.; Chung, Y. C.; Leroi, G. E.; Chang, C. K.; Babcock, G. T. *J. Phys. Chem.* **1987**, *91*, 5887.
(58) Oertling, W. A.; Salehi, A.; Chang, C. K.; Babcock, G. T. *J. Phys. Chem.* **1989**, *93*, 1311.
(59) Li, X-Y.; Czernuszewicz, R. S.; Kincaid, J. R.; Stein, P.; Spiro, T. G. *J. Phys. Chem.* **1990**, *94*, 47.
(60) Li, X.-Y.; Czernuszewicz, Kincaid, J. R.; Su, Y. O.; Spiro, T. G. *J. Phys. Chem.* **1990**, *94*, 31.

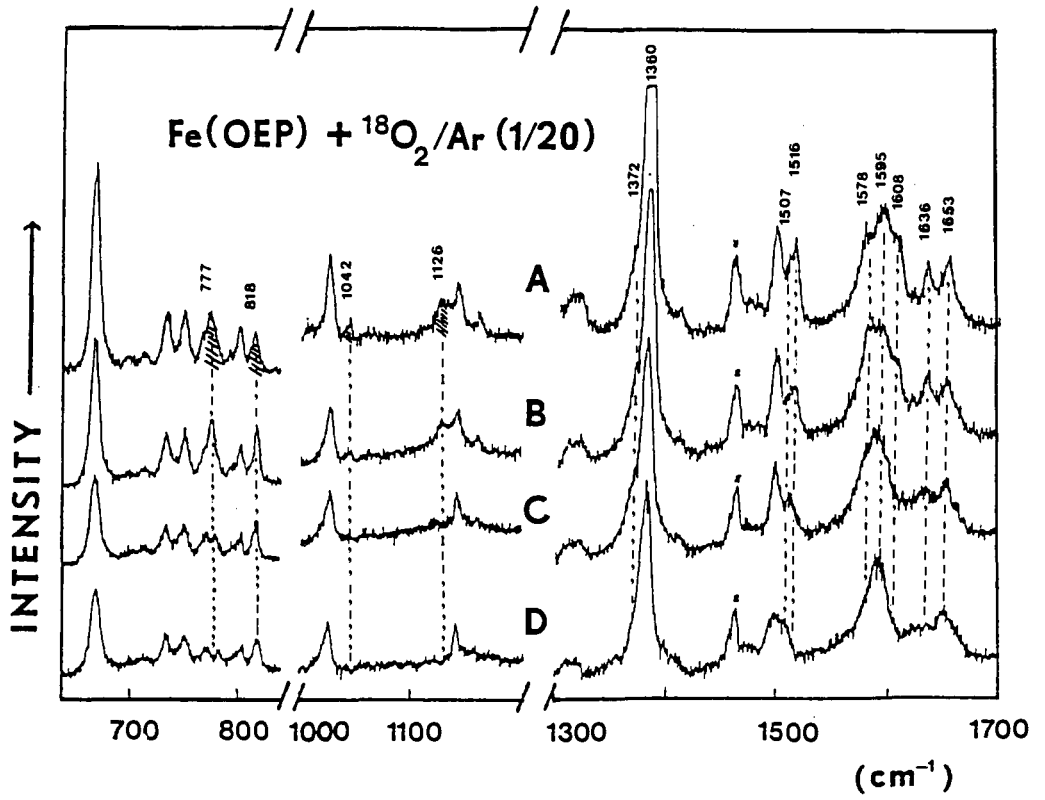

Figure 9. RR spectra of Fe(OEP) cocondensed with $^{18}O_2$/Ar (1:20) at 25 K (406.7-nm excitation): (A) 1.5 mW with 10-min irradiation, (B) 1.5 mW with 30-min irradiation, (C) 2.5 mW with 45-min irradiation, and (D) 6 mW with 90-min irradiation. The marked band at 1463 cm^{-1} is due to the $\nu(O_2)$ of free $^{18}O_2$.

In the high-frequency range, the band at 1578 cm^{-1} exhibits changes in intensity pattern that are similar to that of the 777 cm^{-1} band and is assigned to the ν_2 vibration of the oxoferryl porphyrin in question.

These trends together with complete band assignments available for OV(OEP) and its π-cation radical[61] have been utilized to make band assignments of the high-frequency spectra shown in Table III. As shown earlier,[61] downfield shifts of the ν_2 and ν(FeO) relative to the parent complex are characteristic of an a_{2u} π-cation radical. Thus, we conclude that OFe(OEP$^{\bullet+}$) formed in an O_2 matrix is an a_{2u} π-cation radical. Although this result seems contradictory to other studies that show that M(OEP) complexes tend to form a_{1u} radicals,[56] it should be born in mind that the a_{1u} and a_{2u} states are generally mixed and that the symmetry of the π-cation radical can be temperature-dependent due to a thermal equilibrium between these states.[62,63] Thus, OFe(OEP$^{\bullet+}$) may be an a_{2u} type at 30 K in O_2 matrices. It should be noted that the ν(FeO) (802 cm^{-1}) of OFe(TMP$^{\bullet+}$) (a_{2u} type) in CH_2Cl_2 (−78 °C)[29] is close to that observed in O_2 matrices (809 cm^{-1}) and that its high-frequency-marker bands exhibit shift patterns similar to those of OFe(OEP$^{\bullet+}$) in O_2 matrices upon π-cation radical formation.[28] Thus, we conclude that unstable oxoferryl porphyrins formed in O_2 matrices exhibiting characteristic ν(FeO) at ~810 cm^{-1} assume a π-cation radical form of an a_{2u} type.

(7) Mechanisms for Formation of Oxoferryl Porphyrins in O_2 Matrices. Thus far, oxoferryl porphyrin π-cation radicals have been prepared by chemical[64-66] and electrochemical methods.[65,67]

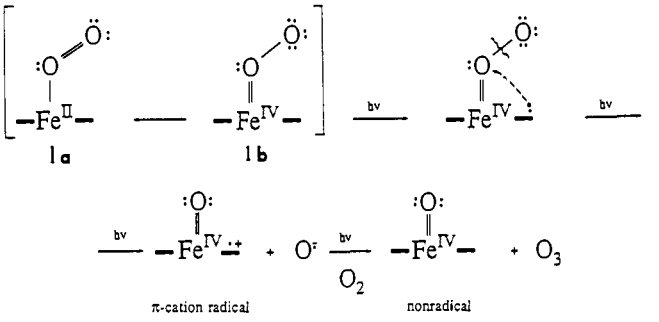

Figure 10. Proposed mechanism for the formation of π-cation radical and nonradical ferryl porphyrins in O_2 matrices.

This work demonstrates, however, that they can also be prepared by photolysis of the corresponding dioxygen adducts in O_2 matrices. Figure 10 illustrates the most probable mechanism for this process. Here, the electronic structure of the FeO_2 moiety is expressed by two resonance structures.[68] In Ia, the shared electron pair in the Fe–O_2 bond is assigned to the more electronegative oxygen atom (cannonical form, Fe(II)O_2), leaving the Fe atom in the +2 state and the O_2 neutral. In Ib, a double bond is formed between the Fe and one of the oxygen atoms, leaving the Fe in the +4 state and the O_2 in a "peroxo-like" state (O_2^{2-}) (cannonical form, Fe(VI)O_2^{2-}). These dioxygen adducts are photolabile, and laser irradiation in the violet range (406–415 nm) induces homolytic cleavage of the O–O bond, which produces an oxoferryl porphyrin π-cation radical and an oxygen anion radical O$^{\bullet-}$. It is clear from Figure 10 that, in order to keep a neutral charge of the Fe(IV)=O bond formed in this photoreaction, one electron from the porphyrin ligand must be shifted to the iron orbitals. Since the O$^{\bullet-}$ immediately reacts with O_2 in an O_2 matrix, it produces ozone (O_3) and an electron:

(61) Macor, K. A.; Czernuszewicz, R. S.; Spiro, T. G. *Inorg. Chem.* **1990**, *29*, 1996.
(62) Morishima, I.; Takamuki, Y.; Shiro, Y. *J. Am. Chem. Soc.* **1984**, *106*, 7666.
(63) Rachlewicz, K.; Latos-Grazynski, L. *Inorg. Chim. Acta* **1988**, *144*, 213.
(64) Groves, J. T.; Haushaiter, R. C.; Nakamura, M.; Nemo, T. E.; Evans, B. J. *J. Am. Chem. Soc.* **1981**, *103*, 2884.
(65) Hickman, D. L.; Nanthakumar, A.; Goff, H. M. *J. Am. Chem. Soc.* **1988**, *110*, 6389.
(66) Balch, A. L.; Latos-Grazynski, L.; Renner, M. W. *J. Am. Chem. Soc.* **1985**, *107*, 2903.
(67) Coldwood, T. S.; Bruce, T. C. *Inorg. Chem.* **1986**, *25*, 3722.
(68) (a) Pauling, L. *Nature* **1964**, *203*, 182. (b) Jones, R. D.; Summerville, D. A.; Basolo, F. *Chem. Rev.* **1979**, *79*, 139.

$$O^{\bullet-} + O_2 \rightarrow O_3 + e$$

This electron reduces the π-cation radical to the nonradical oxoferryl porphyrin, which is fairly stable in low-temperature O_2 matrices. This mechanism accounts for the results shown in Figure 5A and 5B. Namely, the ν(FeO) of the π-cation radical (815 cm^{-1}) becomes weaker, whereas that of the nonradical oxoferryl porphyrin (853 cm^{-1}) becomes stronger as the irradiation time is increased. In contrast to the results presented above, formation of nonradical oxoferryl porphyrins in solution proceeds via a different route.[38]

$$\text{Fe(II)(por)} \xrightarrow{O_2} \text{Fe(Por)}O_2 \xrightarrow{O_2} \text{(por)Fe(III)OOFe(III)(por)} \rightarrow \text{OFe(IV)(por)}$$

In solution at low temperature, Fe(II)(por) reacts with O_2 to form an oxygen adduct, which immediately converts to a more stable μ-peroxo-bridged species $[(por)Fe(III)]_2O_2$. Its formation has been confirmed by the observation of the ν_s(Fe–O) at 574 cm^{-1} in toluene at ~190 K.[38] Such a dimer cannot be formed in an O_2 matrix since Fe(por)O_2 is surrounded by a large excess of O_2 molecules and frozen at 25 K. When the temperature of the solution is raised to ~220 K, the O–O bond of the peroxo dimer is cleaved homolytically and the nonradical oxoferryl porphyrin is formed without an intermediate species such as an oxoferryl porphyrin π-cation radical.

Acknowledgment. This research was supported by the National Science Foundation (Grant DMB-8613741). L.M.P. acknowledges partial support from the Polish Ministry of Education (Grant RP-II-13). We thank Prof. Roman S. Czernuszewicz of the University of Houston for his valuable comments.

Cation Solvation in Nafion/Cu^{2+} Swollen by Acetonitrile from Multifrequency ESR and Simulations

Janusz Bednarek† and Shulamith Schlick*

Contribution from the Department of Chemistry, University of Detroit, Detroit, Michigan 48221.
Received October 1, 1990

Abstract: The gradual replacement of oxygen ligands around Cu^{2+} with nitrogen ligands in Nafion soaked with acetonitrile has been deduced from ESR spectra at L-, S-, C-, and X-bands and from computer simulations. Results suggest that after one cycle of drying and soaking of the membranes with acetonitrile, Cu^{2+} has two ^{14}N ligands in CH_3CN and *none* in CD_3CN. The isotope effect is assigned to the difference in the solvation energies of the sulfonic groups and of cations with deuteriated and protiated solvents and is similar to the recently published preferential solvation of Nafion salts by H_2O compared with D_2O. After two cycles of drying and soaking with the solvents, all four oxygen ligands in the equatorial plane of Cu^{2+} are replaced by nitrogen ligands. The components of the ^{14}N superhyperfine tensor have been deduced, taking into consideration the *apparent* tensor values calculated from the analysis of the splitting from parallel and perpendicular signals of ^{63}Cu. Multifrequency ESR spectra allow determination of all ESR parameters: Spectra at X-band are very important for deducing the **g**-tensor components; spectra at C-band are critical for the determination of the ratio $\delta g/\delta A$ of the distribution parameters due to strain; the greater resolution for the signals corresponding to $m_I = -3/2$ and $-1/2$ at C-band, to $m_I = -3/2$ at X-band, and to $m_I = -1/2$ at S-band is crucial for determining the many parameters involved in the simulation of experimental results. We emphasize the importance of ESR at frequencies *lower* than the usual X-band, for the analysis of disordered systems, in the presence of strain.

I. Introduction

The local environment of paramagnetic cations can be deduced from electron spin resonance (ESR) spectra, based on the **g** tensor and the hyperfine coupling constants of the central cation and on the line widths and line shapes of the signals. The interaction with magnetic ligands is sometimes detected as a line broadening and, in favorable cases, as resolved superhyperfine splittings (shf); this is the case for nitrogen ligands. Detection of shf is very important, because it reflects *directly* the number and symmetry of the ligands around the paramagnetic cation.

Most ESR spectra are taken at a frequency of about 9 GHz, because of convenient sample size and availability of spectrometer. Multifrequency ESR has proven beneficial for both the quality and quantity of information that can be obtained. The optimal frequencies are system dependent: Spectra at 35 GHz (Q-band) are used to increase the separation (in Gauss) when more than one species, differing in **g** values, are present. In recent years however it has become evident that microwave frequencies *lower* that 9 GHz are frequently the best choice, especially in disordered systems, where local structural inhomogeneities ("strain") lead to a distribution in the **g** and hyperfine tensors and cause considerable line broadening.[1]

A model that describes the line widths in the ESR spectra of Cu^{2+} complexes as a function of microwave frequency and m_I values has been suggested by Froncisz and Hyde.[2] The distribution widths of the parallel component of the **g** tensor and of the hyperfine tensor from the central cation, δg and δA, respectively, can be deduced from experimental spectra by using this dependence. For typical values of the distribution parameters, the model predicts increased resolution at lower frequencies; in particular the $m_I = -1/2$ signal is expected to be narrowest at a frequency of ≈2 GHz. This behavior has been verified in a number of biologically important Cu^{2+} complexes, where the advantage of multifrequency ESR has been convincingly demonstrated.[3,4]

* Author to whom correspondence should be addressed.
† On leave from the Institute of Applied Radiation Chemistry, Technical University of Lodz, Lodz, Poland.

(1) Hyde, J. S.; Pasenkiewicz-Gierula, M.; Basosi, R.; Froncisz, W.; Antholine, W. E. *J. Magn. Reson.* **1989**, *82*, 63.
(2) Froncisz, W.; Hyde, J. S. *J. Chem. Phys.* **1980**, *73*, 3123.
(3) Hyde, J. S.; Antholine, W. E.; Froncisz, W.; Basosi, R. In *Advanced Magnetic Resonance Techniques in Systems of High Molecular Complexity*; Niccolai, N., Valensin, G., Eds.; Birkhausen: Boston, 1986; p 363.
(4) Rakhit, G.; Antholine, W. E.; Froncisz, W.; Hyde, J. S. *J. Inorg. Biochem.* **1985**, *25*, 217.

0002-7863/91/1513-3303$02.50/0